HORSESHOE PERIODIC ORBITS WITH ONE SYMMETRY IN THE GENERAL PLANAR THREE-BODY PROBLEM

Abimael Bengochea and Manuel Falconi

Departamento de Matemáticas
Facultad de Ciencias, UNAM
Ciudad Universitaria, México, D.F. 04510

Ernesto Pérez-Chavela

Departamento de Matemáticas
UAM Iztapalapa
Av. San Rafael Atlixco 186, México, D.F. 09340

Abstract. Using collinear reversible configurations and some properties of symmetry we obtain horseshoe periodic orbits in the general planar three-body problem with masses $m_1 \gg m_2 \geq m_3$, which usually represents a system formed by a planet and two small satellites; for instance, the system Saturn-Janus-Epimetheus. For the numerical analysis we have taken the values $m_2/m_1 = 3.5 \times 10^{-4}$ and $m_3/m_1 = 9.7 \times 10^{-5}$ corresponding to 10^5 times the mass ratios of Saturn-Janus and Saturn-Epimetheus, respectively.

1. **Introduction.** In the classical three-body problem there are several kinds of families of periodic orbits, the well known Euler and Lagrange relative equilibria, the figure eight orbits, the Shubart orbits (periodic orbits with binary collisions) and the horseshoe periodic orbits among many others.

A mechanism which generates these kind of orbits appears when, for instance, we find co-orbital trajectories in a system formed by a big planet and two small moons orbiting around it on very similar trajectories. The masses of the moons are similar, so that at the close *encounter* between them, there is a significant influence on each other which permits avoid the collision, and the moons interchange trajectories; the inner body becomes outer and vice versa until the next close *encounter* where the same phenomena occurs and so on. In a rotating frame with an adequate constant angular velocity the shape of the moons trajectories looks like a horseshoe.

Several people have studied the horseshoe orbits, usually they start their analytical analysis with the study of the restricted three-body problem. Some of the approaches that they have used are a combination of perturbation theory and numerical integration [5, 6], an analytic approximation to the motion around the planet in resonance 1 : 1 [17, 18], a singular perturbation treatment because of the

regions of small or big interaction between the satellites [16], [19], or a theoretical and numerical approach in the Hill's model [14], [8]. In the general model, this problem has been studied by means of introducing small parameters in the equations of motion and the retention of the dominant part in order to obtain dynamical information of the system [4], or as an adiabatic perturbation of the classical equilateral triangle Lagrange solution and of the collinear Euler solution [2]. The existence of stable planar horseshoe periodic orbits for the Saturn-Janus mass parameter in the restricted circular three-body problem has been proved in [11]. Also in the restricted circular three-body problem, in [1] were determined families of periodic orbits of horseshoe type, for the planar and spatial case. In the same model, in [9] were studied some properties of the symmetric horseshoe periodic families according to their bifurcation features.

This paper is the continuation of a study of horseshoe periodic orbits in the general planar three-body problem [3], which we refer as Paper I. In that study we considered horseshoe orbits with two equal masses, for a mass ratio equals 3.5×10^{-4}. The symmetric horseshoe periodic orbits were determined by means of reversible properties of the equations of motion. We focused on the horseshoe orbits that pass through two reversible configurations, namely collinear and isosceles, or in other words horseshoe orbits of type collinear-isosceles (at this point we must remark that the isosceles reversible configuration only exists if at least two of the three masses of the bodies are equal). These horseshoe periodic orbits display two symmetries in the rotating frame.

In this paper we show the existence of horseshoe orbits for mass ratios $m_2/m_1 = 3.5 \times 10^{-4}$, $m_3/m_1 = 9.7 \times 10^{-5}$, nevertheless this procedure can be applied to other problems (for instance the Saturn-Janus-Epimetheus system). We have used similar tools as Paper I, but here we do not have an isosceles reversible configuration any more, so we have managed the problem using a collinear reversible configuration. In other words, we study those horseshoe orbits which start at a collinear reversible configuration and after some time reach a configuration of the same type. Some families of the periodic orbits (in the sense of the Cylinder Theorem; see p. 136 in [12]) that we find are similar to the ones found using collinear and isosceles reversible configurations, but in addition, in this paper we also find families of periodic orbits with different behavior.

The paper is organized as follows: In Section 2 we describe the planar horseshoe motion and we give the equations of motion of the three-body problem. In Section 3 we study the orbits which start at a collinear reversible configuration and reach another collinear reversible configuration. In Section 4 we present the procedure to obtain horseshoe orbits which pass through two collinear reversible configurations as we pointed out in Section 3. We also give the numerical results. We finish the paper with the conclusions of this work.

2. **Description of the planar horseshoe motion and equations of motion.** We consider three point particles that by short we call as particles 1, 2, 3 with corresponding masses $m_1 >> m_2 \geq m_3$, whose motion takes place in a fixed plane. Usually, it is said that 1 is the primary body or planet, and 2 and 3 are called satellites or minor bodies.

2.1. **Horseshoe motion. Circular case.** We begin at a point P of the orbit where the three bodies are aligned with the particle of mass m_1 between the other two. Since we are considering that the planet has a significantly bigger mass than

the corresponding of the satellites, the description also applies to a frame of reference with origin at the center of mass of the three bodies.

Close to the point P, the interaction between the satellites is negligible and their motions are dominated by the force exerted by the primary body, then the trajectory of each satellite is approximately elliptic. Nevertheless, for this case we assume that the eccentricities of the elliptic motions are zero. At the starting point P, we consider that the semimajor axis associated to the particle 3 is smaller than the corresponding to 2, and therefore it is said that 3 is in an inner orbit, and 2 is an outer orbit. The satellites go around the primary and eventually the distance between the satellites decreases and their interaction is not longer negligible. Due to this strong interaction, a change in the orbits occur: 3 follows an outer orbit, and 2 an inner one. It means that a close *encounter* between the satellites has happened. An important feature during the exchange of orbits is that the alignment of the three bodies does not occur. After that, the separation between them will increase until the three bodies reach an alignment where 2 is the inner body and 3 is the outer one, and the process is repeated, interchanging 2 and 3 in the above discussion. The evolution of this orbit is shown in Figure 1. The whole orbit can be seen in a rotating frame with an adequate constant angular velocity. In this frame of reference the trajectory of each satellite takes the form of a smooth horseshoe, and its size depends on the mass ratio of the satellites, as is shown in Figure 2. Notice that during a "horseshoe cycle" (rotating frame), the orbit passes only through two alignments; it is outlined in items (a) and (c) of Figures 1 and 2.

2.2. Horseshoe motion. Non-circular case.

In the previous description we have assumed that in some part of the orbit of the three bodies the trajectory of each satellite can be approached by a circular one, that is, the osculating eccentricities of the satellites' orbits are close to zero. Now, if instead of that we consider non-zero osculating eccentricities (but small, in order to keep the horseshoe shape), new features appear:

- In the rotating frame the trajectory of each satellite is also horseshoe shaped, but now it is formed by many curls; each one corresponds to one revolution around the planet by the satellite.
- The horseshoe orbit may pass through consecutive alignments. That is, more than two alignments in a "horseshoe cycle", on which the temporal separation between neighboring alignments is less than half of the time required by any of the minor bodies to go once around the planet (this point will be revisited in Section 4).

According to the description given above, we could define the horseshoe motion in the following way. Consider two minor bodies 2, 3 orbiting around a primary body 1, and denote the angle (non constant) between the minor bodies at time t, measured in counterclockwise sense with origin at 1, by $\theta_{23}(t)$. If there is no overtake between the minor bodies for any time, that is $\theta_{23}(t) \neq 0 \bmod 2\pi$, $t \in \mathbb{R}$, we say that the orbit of the three bodies is of horseshoe type.

Consider particles 1, 2, 3 with masses m_1, m_2, m_3, and the planar vectors of position, and velocity

$$\mathbf{r}_i = \begin{pmatrix} x_i \\ y_i \end{pmatrix}, \quad \mathbf{v}_i = \dot{\mathbf{r}}_i, \ \ i = 1, 2, 3,$$
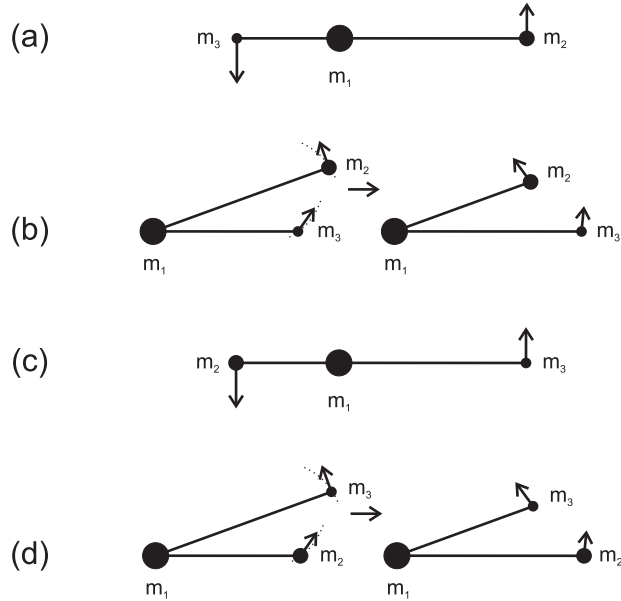
FIGURE 1. Evolution of the horseshoe orbit. (a) Initial alignment with the body 3 in an inner orbit. (b) Interchange of orbits during the *encounter*. (c) Second alignment with the body 2 in an inner orbit. (d) The *encounter* after the alignment in (c).
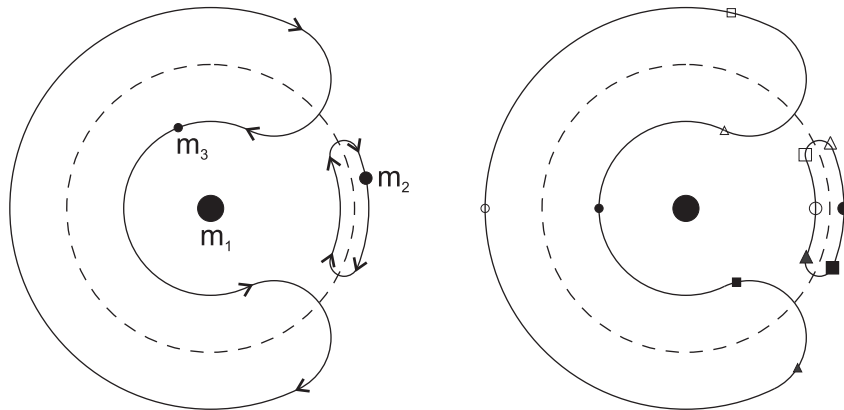

FIGURE 2. Horseshoe orbits in a rotating frame with constant angular velocity, for the mass ratio $m_2/m_3 = 4$. At the right side are indicated the six configurations that make up the Figure 1. It was used a symbol per configuration. The correspondence is as follows: (a) bold circle, (b)$_1$ bold square, (b)$_2$ bold triangle, (c) blank circle, (d)$_1$ blank square and (d)$_2$ blank triangle.

in an inertial frame. The kinetic energy of the system is

$$T = \frac{1}{2} \sum_{i=1}^{3} m_i \mathbf{v}_i^2,$$

and the gravitational potential is

$$U = -\frac{Gm_2m_3}{r_{23}} - \frac{Gm_3m_1}{r_{31}} - \frac{Gm_1m_2}{r_{12}},$$

where G is the universal gravitational constant, and $r_{ij} = |\mathbf{r}_i - \mathbf{r}_j|$ denotes the distance between the bodies i and j. The equations of motion are defined by the Lagrangian of the system

$$L = T - U,$$

by means of the Lagrange equations

$$\frac{d}{dt}\frac{\partial L}{\partial \dot{\mathbf{r}}_i} - \frac{\partial L}{\partial \mathbf{r}_i} = \mathbf{0}, \quad i = 1, 2, 3. \tag{1}$$

After some computations (1) becomes

$$\ddot{\mathbf{r}}_1 = \frac{Gm_2(\mathbf{r}_2 - \mathbf{r}_1)}{r_{12}^3} + \frac{Gm_3(\mathbf{r}_3 - \mathbf{r}_1)}{r_{31}^3},$$

$$\ddot{\mathbf{r}}_2 = \frac{Gm_3(\mathbf{r}_3 - \mathbf{r}_2)}{r_{23}^3} + \frac{Gm_1(\mathbf{r}_1 - \mathbf{r}_2)}{r_{12}^3},$$

$$\ddot{\mathbf{r}}_3 = \frac{Gm_1(\mathbf{r}_1 - \mathbf{r}_3)}{r_{31}^3} + \frac{Gm_2(\mathbf{r}_2 - \mathbf{r}_3)}{r_{23}^3}.$$

3. **Reversible configurations and periodic motions.** In the study of periodic orbits in the n-body problem is often useful to consider the time-reversal symmetry of the equations of motion [10]. For our purpose we precise the following terms: given a planar orbit in an inertial frame we say that the configuration of the bodies is collinear if their positions lie on a common line at a certain time, and in addition is called reversible if the velocities are perpendicular to the direction of the alignment. We measure the reversible configurations modulo rotations, that is, if $\mathbf{r}_i$, $\mathbf{v}_i$, $i = 1, 2, 3$ defines a collinear reversible configuration then $R\mathbf{r}_i$, $R\mathbf{v}_i$, $i = 1, 2, 3$, where R is any rotation, specifies the same configuration.

In the case of n bodies, the periodicity of orbits which pass through two collinear reversible configurations has been studied in [15], which is applicable to our model. In Paper I [3], for the study of horseshoe periodic orbits with two equal masses, together with collinear reversible configurations, we have used isosceles reversible configurations, which exist if at least two of the three masses are equal to each other. Any orbit which passes through a reversible configuration has an interesting property: the part of the orbit previous to the reversible configuration is related with the posterior one by means of a linear transformation.

In the following we will show under what conditions an orbit (not necessarily of horseshoe type) which passes through two collinear reversible configurations is periodic (unless otherwise stated, we refer to periodicity in the inertial frame). From here on we consider a frame of reference with origin at the center of mass of the three bodies.

Theorem 3.1. *Consider an orbit of three bodies* $\mathbf{r}_i(t)$, $i = 1, 2, 3$, $t \in \mathbb{R}$, *with collinear reversible configurations at times* $t = 0$, $t = T_\theta$. *Define* θ *as the angle measured from the vector* $\mathbf{r}_2(0)$ *to* $\mathbf{r}_2(T_\theta)$ *in the counterclockwise sense. The orbit is periodic if and only if*

$$\theta = \frac{p}{q}\pi, \quad \text{for some } p, q \in \mathbb{N}.$$

If p and q are relative primes, the period of the orbit T is

$$T = 2qT_\theta.$$

Proof. Consider an inertial frame such that $\mathbf{r}_2(0)$ lies on the x axis, at the positive side. Given a counterclockwise rotation R_θ, we introduce a primed frame of reference by means of

$$\mathbf{s}' = R_{-\theta}\mathbf{s}.$$

Since we have a collinear reversible configuration on the x' axis at $t = T_\theta$, we get the equations (for details see appendix)

$$\mathbf{r}'_i(t) = K\mathbf{r}'_i(2T_\theta - t), \ \ i = 1, 2, 3, \ \ t \in \mathbb{R},$$
$$\mathbf{v}'_i(t) = -K\mathbf{v}'_i(2T_\theta - t), \ \ i = 1, 2, 3, \ \ t \in \mathbb{R}, \tag{2}$$

with

$$K = \begin{pmatrix} 1 & 0 \\ 0 & -1 \end{pmatrix}.$$

In terms of the coordinate system (x, y) the relation (2) becomes

$$\mathbf{r}_i(t) = R_{2\theta}K\mathbf{r}_i(2T_\theta - t), \ \ i = 1, 2, 3, \ \ t \in \mathbb{R},$$
$$\mathbf{v}_i(t) = -R_{2\theta}K\mathbf{v}_i(2T_\theta - t), \ \ i = 1, 2, 3, \ \ t \in \mathbb{R}, \tag{3}$$

where it was used $KR_{-\theta} = R_\theta K$. Due to the collinear reversible configuration at $t = 0$ we have $K\mathbf{r}_i(0) = \mathbf{r}_i(0)$, $-K\mathbf{v}_i(0) = \mathbf{v}_i(0)$, $i = 1, 2, 3$. Thus, at $t = 2T_\theta$ the solution (3) takes the form

$$\mathbf{r}_i(2T_\theta) = R_{2\theta}\mathbf{r}_i(0), \ \ i = 1, 2, 3,$$

$$\mathbf{v}_i(2T_\theta) = R_{2\theta}\mathbf{v}_i(0), \ \ i = 1, 2, 3.$$

Notice that the collinear reversible configurations of the three bodies at $t = 0$ and at $t = 2T_\theta$ are equal to each other, and that their angles with respect to the horizontal axis are 0, 2θ respectively. Since the system is invariant under rotations, it follows

$$\mathbf{r}_i(2T_\theta + t) = R_{2\theta}\mathbf{r}_i(t), \ \ i = 1, 2, 3, \ \ t \in \mathbb{R},$$
$$\mathbf{v}_i(2T_\theta + t) = R_{2\theta}\mathbf{v}_i(t), \ \ i = 1, 2, 3, \ \ t \in \mathbb{R}. \tag{4}$$

Using (4) we get

$$\mathbf{r}_i(2mT_\theta + t) = R_{2m\theta}\mathbf{r}_i(t), \ \ i = 1, 2, 3, \ \ m \in \mathbb{Z}, \ \ t \in \mathbb{R},$$

and the same happens for the velocities.

The angle θ determines the periodicity of the orbit, whereas the pair (θ, T_θ) defines the period. A necessary and sufficient condition for the periodicity is

$$\theta = \frac{p}{q}\pi, \ \text{ for some } \ p, q \in \mathbb{N}. \tag{5}$$

The period T of the orbit can be calculated considering the irreducible form of the fraction that appears in the relation (5). If p and q are relative primes, then

$$T = 2qT_\theta.$$

$\square$

In Figure 3 are outlined the first three collinear reversible configurations of the above process.
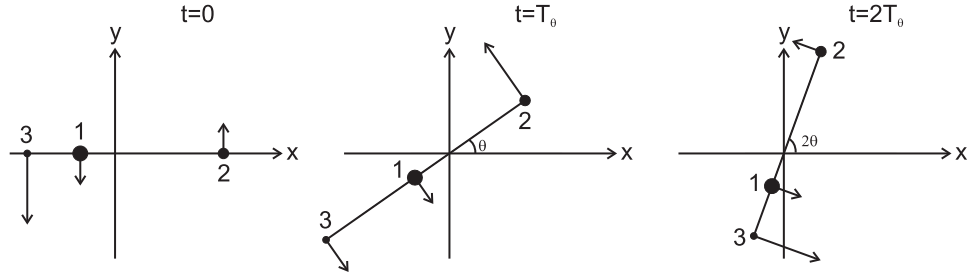

FIGURE 3. Collinear reversible configurations in an inertial frame of reference with origin at the center of mass of the three bodies.

Using the equations (3) and (4), some properties of the orbits can be obtained. For example, the shape is $2T_\theta$ periodic (for instance, see [15]) and the relative distances between the bodies present periodicity and symmetry. For any permutation $i, j, k \in \{1, 2, 3\}$, $m \in \mathbb{Z}$, $\Delta \in \mathbb{R}$ holds $r_{ij}(\Delta + 2mT_\theta) = r_{ij}(\Delta)$, $r_{ij}(\Delta + mT_\theta) = r_{ij}(-\Delta + mT_\theta)$.

4. **Numerical study of horseshoe periodic orbits.** Along this section we give the necessary elements to expose a procedure for obtaining horseshoe periodic orbits with different masses. We use it to calculate families of horseshoe periodic orbits, in the sense of the Cylinder Theorem [12], for mass ratios $m_2/m_1 = 3.5 \times 10^{-4}$, $m_3/m_1 = 9.7 \times 10^{-5}$.

Due to its frequent use, we introduce the following notation: we denote by C_i, $i = 2, 3$ a collinear configuration with i as the inner body, and we use RC instead of C if in addition the collinear configuration is reversible. We also use ordered time intervals $I_j \subset \mathbb{R}$ and natural numbers $N_j \geq 1$, for $j \in \mathbb{N}$ (by ordered time intervals we mean the following: suppose we have I_n, I_m with $n > m$, then for all $t \in I_n$, $t^* \in I_m$ holds $t > t^*$). Finally, we denote by Γ an initial condition of type RC_3 (at time $t = 0$, according to section 3) that gives rise to a horseshoe orbit, by S a set of initial conditions of horseshoe orbits which pass through a RC_3 at $t = 0$, and $S_R \subset S$ for the subset which consists of the initial conditions of horseshoe orbits which pass through a RC_2 at T_θ.

Before stating the problem of study, we review the description of a horseshoe orbit (non-zero eccentricities) in terms of C_i, $i = 2, 3$. In a certain time interval I_1 the horseshoe orbit passes through N_1 configurations C_3. After that, an *encounter* happens (3 goes to an exterior orbit and 2 goes to an interior one), and later, in a time interval I_2, the horseshoe orbit passes through N_2 configurations C_2. Subsequently a new *encounter* appears (2 goes to an exterior orbit and 3 goes to an interior one), and later, in a time interval I_3, the horseshoe orbit passes through N_3 configurations C_3, and so on. Notice that these time intervals depend on the orbit.

4.1. **Statement of the problem and solution.** Now we state the problem of numerical study as follows: determine horseshoe periodic orbits which pass through two collinear reversible configurations: RC_3 in I_1 and RC_2 in I_2. Being more precise, RC_3 at $t = 0$ and RC_2 at T_θ. Notice that these horseshoe orbits pass through RC_3, an *encounter*, and RC_2, in $[0, T_\theta]$.

In the following we present, roughly speaking, the main steps to follow in order to obtain horseshoe periodic orbits (in later subsections we give the details of each one). First, reduce the possible initial conditions that lead to RC_3. Second, determine an initial condition Γ which, by definition, is of type RC_3 and defines a horseshoe orbit, not necessarily periodic. To obtain convenient *candidates* for Γ we use an analytical approximation of two decoupled Kepler problems forming a RC_3 at $t = 0$. From here we obtain several initial conditions which, by numerical integration of the corresponding orbits, we examine in order to determine horseshoe orbits. In principle, there exist neighborhoods of Γ that could be used as S. Third, determine the subset $S_R \subset S$, or at least some part of it (for this we introduce the D subsets; their intersections belong to S_R). Finally, the set S_R only has initial conditions of horseshoe orbits which pass through RC_3 at $t = 0$ and RC_2 at T_θ, thus the periodicity of each orbit is determined by the corresponding angle θ, according to Theorem 3.1.

4.2. **Reduction of the space of initial conditions of type RC_3.** Given the masses m_1, m_2, m_3, and choosing an inertial frame of reference with origin at the center of mass of the three bodies, the initial condition x_{i0}, y_{i0}, vx_{i0}, vy_{i0}, $i = 2, 3$ determines RC_3 and the respective orbit. Since the potential is homogeneous we can fix the magnitude of one coordinate; so, we choose $|x_{30}| = 1$, and due to the invariance of the Lagrangian under rotations we can assume that the alignment at the initial time is along the x axis, with 3 at the left, therefore $x_{30} = -1$, $y_{i0} = 0$, $vx_{i0} = 0$, $i = 2, 3$, letting x_{20}, vy_{20}, vy_{30} to be determined. From here on we use without loss of generality Γ and the ordered triple $(x_{20}, vy_{20}, vy_{30})$, and consider S as a subset of a three dimensional space.

4.3. **Initial conditions of type RC_3 for horseshoe orbits.** Since at collinear configurations the interaction between satellites is negligible, for arbitrary mass ratios m_2/m_1, m_3/m_1 (they must be small enough in order to horseshoe motion takes place) we obtain *candidates* for Γ using two decoupled Kepler systems, namely 1-2 and 1-3. For simplicity we consider that in each system the mass of the satellite is negligible, and that the motion of each satellite is circular. Choosing the alignment along the x axis with the second body at positive side, and the evolution of the movement in counterclockwise sense, the initial condition results

$$\tilde{\mathbf{r}}_{10} = \mathbf{0}, \ \tilde{\mathbf{r}}_{20} = \hat{\boldsymbol{\imath}} a_2, \ \tilde{\mathbf{r}}_{30} = -\hat{\boldsymbol{\imath}} a_3, \ \tilde{\mathbf{v}}_{10} = \mathbf{0}, \ \tilde{\mathbf{v}}_{20} = \hat{\boldsymbol{\jmath}}\sqrt{\frac{Gm_1}{a_2}}, \ \tilde{\mathbf{v}}_{30} = -\hat{\boldsymbol{\jmath}}\sqrt{\frac{Gm_1}{a_3}},$$

(6)

where a_i is the semimajor axis of the orbit of the body $i = 2, 3$, and $\hat{\boldsymbol{\imath}}$, $\hat{\boldsymbol{\jmath}}$ denote the usual canonical unit vectors. There are two things to take into account, in order to determine the semimajor axes. First, since (6) must define a RC_3 the third body follows an inner orbit, that is $a_3 < a_2$. Second, in order to get the horseshoe shape of the orbit, the semimajor axes should not be very different between them.

About the initial condition (6), we make relevant comments. For positive masses m_i, $i = 1, 2, 3$, the initial condition (6) does not define a motion in an inertial system with origin at the center of mass of the three bodies, and in general $\tilde{x}_{30} \neq -1$, that is, the initial condition is not "normalized", in the sense of subsection 4.2. To solve this we only have to subtract the corresponding vectors of the center of mass and later use the homogeneity of the potential.

Since the mass ratios m_2/m_1, m_3/m_1 are very similar with the given in Paper I [3] (in fact m_2/m_1 has the same value in both cases), and the corresponding initial

conditions of Paper I define a RC_3 configuration at $t = 0$, we have used these initial conditions as *candidates* for Γ.

Remark 1. If Γ is an initial condition of a horseshoe orbit then, by the Theorem of continuity with respect to initial conditions and parameters, the same happens for the points in a small enough neighborhood of Γ.

4.4. **Algorithms and determination of S_R.** In this section we describe in detail the procedure to obtain a set of initial conditions $S_R \subset S$ of horseshoe orbits which pass through RC_3 at $t = 0$ and RC_2 at $t = T_\theta$.

Let N_2 be the number of configurations C_2 for which a horseshoe orbit passes through in I_2, and $\hat{T}_\theta$ the time when the *ith* configuration C_2 is reached ($1 \leq i \leq N_2$). We define the sets

$$D_{N_2,i,j} = \{(x_{20}, vy_{20}, vy_{30}) \in S \mid \mathbf{r}_j(\hat{T}_\theta) \cdot \mathbf{v}_j(\hat{T}_\theta) = 0\}, \ \ j = 2, 3. \tag{7}$$

A necessary and sufficient condition for $\Gamma \in S$ defines a horseshoe orbit which passes through N_2 configurations C_2, where the *ith* is reversible, is that Γ belongs to $D_{N_2,i,2} \cap D_{N_2,i,3}$ (for the *ith* term holds $C_2 = RC_2$, $\hat{T}_\theta = T_\theta$). We remark that the set S_R is composed of all possible intersections of this type, that is

$$S_R = \bigcup_{N_2,i} D_{N_2,i,2} \cap D_{N_2,i,3}. \tag{8}$$

Depending on S, the sets that appear in the previous equation, or their intersections, may be empty.

4.4.1. *Units, algorithms and determination of $D_{N_2,i,2} \cap D_{N_2,i,3}$.* In the following circular items we introduce choice of units and algorithm for the numerical integration of the orbits. According to subsection 4.3, the evolution of the orbits is chosen in counterclockwise sense.

- For the numerical study we choose units of mass $U_m = m_1$, distance $U_d = d_0$, and time $U_t = t_0 = \sqrt{\frac{d_0^3}{G_0 m_1}}$, where $G = G_0 m^3/s^2 kg$, $G_0 = 6.67 \times 10^{-11}$. Since we are using "normalized" initial conditions (see subsection 4.2), the important point is the relation between d_0 and t_0, not their particular values. In these units $G = 1$.
- Let F be the projection of the vector $\mathbf{r}_3 \times \mathbf{r}_2$ on the $\hat{\boldsymbol{k}}$ direction, that is $F = x_3 y_2 - x_2 y_3$ (its value is zero at collinear configurations). To determine numerically the orbits we consider the algorithm RK54 [7], with double precision variables and tolerance of 1×10^{-12} for the distances and velocities. We start using the adaptive stepsize suggested in the above reference. One step before reaching the configuration C_2 in which we are interested, we control the step size to diminish F, until we get a value less than 1×10^{-12}.

In these units, considering the system of 1 and 3 as a Kepler system, where m_3 is negligible in comparison to m_1, and 3 in a circular orbit, 2π is the time required by the body 3 to go once around the planet.

Before introducing the steps to follow in order to determine $D_{N_2,i,2} \cap D_{N_2,i,3}$ we make two comments. First, for the determination of $D_{N_2,i,2} \cap D_{N_2,i,3}$ it is useful to introduce $Q_j(x_{20}, vy_{20}, vy_{30}) = \mathbf{r}_j(\hat{T}_\theta) \cdot \mathbf{v}_j(\hat{T}_\theta)$, $j = 2, 3$. According to (7), the set $D_{N_2,i,2} \cap D_{N_2,i,3}$ is conformed by the points $(x_{20}, vy_{20}, vy_{30}) \in S$ which meet

$$Q_2(x_{20}, vy_{20}, vy_{30}) = 0, \ \ Q_3(x_{20}, vy_{20}, vy_{30}) = 0. \tag{9}$$

In principle, each equation of (9) defines a two dimensional manifold, thus the solution set has to be a curve in S. Second, concerning to periodicity, we are considering horseshoe orbits which pass through two collinear reversible configurations. These orbits satisfy $\theta_{23}(t) \neq 0 \mod 2\pi$, $t \in \mathbb{R}$ (see definition of horseshoe orbit in subsection 2.2). However, according to Theorem 3.1, the periodicity is related only with collinear reversible configurations, not with the shape of the orbit (by means of θ_{23}). Thus, there is no guarantee that in a whole periodic family all its orbits have horseshoe shape. Evidently, since we have restricted our numerical study to the set S, then by definition, all computed periodic orbits have such shape. In a wider study, for instance the determination of an entire periodic family, you could follow similar steps to those listed below. The only difference is that once you have determined a point of $D_{N_2,i,2} \cap D_{N_2,i,3}$ (the corresponding orbit has a horseshoe shape), that is the *seed* for the periodic family, you must drop the restriction $\theta_{23}(t) \neq 0 \mod 2\pi$, $t \in \mathbb{R}$ for the subsequent orbits.

Now we describe the steps to follow in order to obtain $D_{N_2,i,2} \cap D_{N_2,i,3}$, thus some part of S_R.

1. Determine $\Gamma = (x_{20}, vy_{20}, vy_{30})$, that is, an initial condition of a horseshoe orbit which forms a RC_3 at $t = 0$. With this, we have implicitly a set of initial conditions S.

2. Pick k_1 initial conditions for different values of the second coordinate, that is $(x_{20}, vy_{20} + n_1\Delta_2, vy_{30}) \in S$ for $n_1 = 1, 2, 3, \cdots, k_1$, and a small enough $\Delta_2 \in \mathbb{R}$, and follow each orbit until the *ith* configuration C_2. Check the quantities $Q_j = \mathbf{r}_j(\hat{T}_\theta) \cdot \mathbf{v}_j(\hat{T}_\theta)$, $j = 2, 3$; if a change of sign occurs in Q_j for consecutive initial conditions we have identified approximately a point of $D_{N_2,i,j}$ (we take the average of these consecutive initial conditions to represent such point), consequently $D_{N_2,i,j}$. In the numerical analysis, we used the points which give rise to $|Q_j| < 1 \times 10^{-12}$ as for $D_{N_2,i,j}$.

3. Check the difference between all the points $\Gamma_2 \in D_{N_2,i,2}$ and $\Gamma_3 \in D_{N_2,i,3}$, that is $\Gamma_2 - \Gamma_3$, since we are interested in $D_{N_2,i,2} \cap D_{N_2,i,3}$. Identify some of the pairs with minimum distance and pick one of them. If the selected pair $\Gamma_{20} = (x_{20}, vy'_{20}, vy_{30})$, $\Gamma_{30} = (x_{20}, vy''_{20}, vy_{30})$ leads to $|vy'_{20} - vy''_{20}| < 2\Delta_2$ then reduce Δ_2 and perform a better approximation of Γ_{20} and Γ_{30}. For the next computations we can use the same value (or less) of Δ_2.

4. Repeat the second step for $\Gamma_{20} + (0, 0, n_2\Delta_3)$, $\Gamma_{30} + (0, 0, n_2\Delta_3) \in S$ where $n_2 = -k_2, -k_2 + 1, \cdots, k_2 - 1, k_2$, for some $k_2 \in \mathbb{N}$, and a small enough $\Delta_3 \in \mathbb{R}$. Considering only terms with the same index at a time, determine pairs "originating" from Γ_{20}, Γ_{30}, namely $\Gamma_{20,n_2} = (x_{20}, vy'_{20,n_2}, vy_{30,n_2}) \in D_{N_2,i,2}$, $\Gamma_{30,n_2} = (x_{20}, vy''_{20,n_2}, vy_{30,n_2}) \in D_{N_2,i,3}$. Finally, make the sequence conformed by the difference of each pair, being n_2 the index; it is enough to consider only the second coordinate, that is $vy'_{20,n_2} - vy''_{20,n_2}$. If a change of sign occurs in consecutive terms, namely n'_2 and $n'_2 + 1$, we have identified approximately a point of $D_{N_2,i,2} \cap D_{N_2,i,3}$, for instance $(\Gamma_{20,n'_2} + \Gamma_{30,n'_3})/2$. If the chosen pair is not useful then select one of its two adjacent pairs and back to the step 3.

5. Apply the second and fourth steps to Γ_{20,n'_2}, Γ_{30,n'_3}, with lower values Δ_2, Δ_3, to get a better approximation of the intersection. For the numerical analysis we have used $\Gamma = (\Gamma_2 + \Gamma_3)/2$, with $|\Gamma_2 - \Gamma_3| < 1 \times 10^{-12}$ as points of $D_{N_2,i,2} \cap D_{N_2,i,3}$.

6. Once determined a point $(x_{20}, \hat{v}y_{20}, \hat{v}y_{30}) \in D_{N_2,i,2} \cap D_{N_2,i,3}$, use $x'_{20} = x_{20} + \Delta_1$, for some small enough $\Delta_1 \in \mathbb{R}$, instead of x_{20}, and repeat the above steps, until to get a new point $(x'_{20}, \hat{v}y'_{20}, \hat{v}y'_{30}) \in D_{N_2,i,2} \cap D_{N_2,i,3}$. If the new pair Γ_{20}, Γ_{30} of the third step is close enough to $(x_{20}, \hat{v}y_{20}, \hat{v}y_{30})$, then $(x_{20}, \hat{v}y_{20}, \hat{v}y_{30})$ and $(x'_{20}, \hat{v}y'_{20}, \hat{v}y'_{30})$ belong to the same branch of $D_{N_2,i,2} \cap D_{N_2,i,3}$.

According to (8), if $D_{N_2,i,2} \cap D_{N_2,i,3} \neq \emptyset$ then some part of S_R has been determined. Evidently, repeating the previous process for new values N_2, i, a more complete set S_R could be obtained. Once we have obtained S_R, the angle θ of the corresponding horseshoe orbits determines the periodicity, according to Theorem 3.1. Such Theorem shows that $\theta/\pi \in \mathbb{Q}$ is a necessary and sufficient condition for the periodicity of the orbit. Nevertheless, in a numerically sense, the case $\theta/\pi \in \mathbb{I}$ is also represented by the other one, due to the finite precision of the numerical calculations. Thus, at least numerically, the most interesting horseshoe periodic orbits are those where the corresponding quotient θ/π is a "simple" fraction, for instance $1/2$ or $2/3$.

4.5. Numerical results.

According to the previous subsection, the initial conditions in $D_{N_2,i,2} \cap D_{N_2,i,3}$ define horseshoe orbits which pass through N_2 configurations C_2 in I_2, with the *ith* term reversible. In terms of $F = x_3y_2 - x_2y_3$, each C_2 corresponds to a root, that is for these motions F has N_2 roots in I_2. Nevertheless, we are only interested in the root corresponding to RC_2, that is the *ith* root. We shall refer to such root according to its temporal appearance: first, second, $\cdots$, or for short root i. Once the root is specified, we use T_θ to denote the time that the three bodies need to come from RC_3 to RC_2.

The function F has a similar structure for any horseshoe orbit. In figure 4 is shown an example of the function F over the time interval $[0, 2T_\theta)$, which covers the whole shape of the horseshoe orbit. In Figures 5 and 6 we have plotted enlargements of F for the cases of one and three roots, respectively.

We have studied a region S which provides up to three consecutive roots in I_2. In order to use (8) for the determination of S_R, it is necessary to distinguish all possible values of N_2 and i. For our case we have $(N_2, i) = (1, 1), (2, 1), (2, 2), (3, 1), (3, 2), (3, 3)$. From the numerical analysis we have obtained that only $(N_2, i) = (1, 1), (3, 2)$ lead to non-empty intersections, then we focus on them.

The numerical study shows that in the studied region S each set $D_{N_2,i,2}$ or $D_{N_2,i,3}$, $(N_2, i) = (1, 1), (3, 2)$ is conformed approximately by several parallel flat surfaces, then the intersection $D_{N_2,i,2} \cap D_{N_2,i,3}$ looks like a set of straight lines with the same inclination. On each straight line $l(x_{20}, vy_{20}, vy_{30})$ the points which generates orbits with $\theta/\pi \in \mathbb{Q}$ form a family of periodic orbits $\widehat{\mathcal{P}}$. Notice that S is small (for reference see Figures 7 and 8); it could lead to the appearance of such patterns (flat or linear). In principle, except for a situation of bifurcation (see Figure 15 and related paragraph), it is expected that for all orbits within a whole periodic family the corresponding numbers N_2, i do not change, that is, are constant in the entire periodic family.

To classify the periodic families $\widehat{\mathcal{P}}$, in addition to N_2, i, it is necessary one more label; we use the number n of complete revolutions that, in a horseshoe orbit, the second body gives around the planet while the three bodies come from RC_3 to RC_2. We remark that n does not change in a common periodic family defined on S, which is the case studied along this paper. We observe that if we continue the periodic
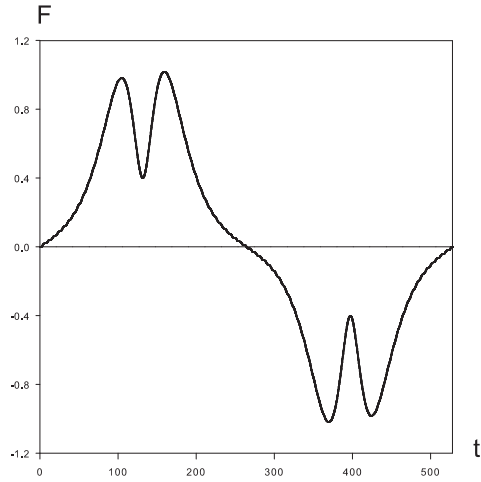
FIGURE 4. Temporal evolution of F corresponding to the orbit $O(1, 41, 0.9997)$, $2T_\theta \approx 528$ (for notation see subsection 4.5).
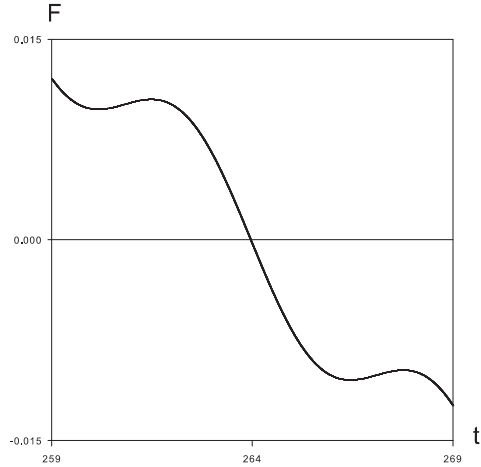

FIGURE 5. An amplified view of F of the orbit $O(1, 41, 0.9997)$, $T_\theta \approx 264$.

family beyond S then such property could not hold, since the second body might complete more revolutions in the new orbits; in this case n would require a slight modification. To simplify the notation we omit N_2, since each case can be identified with the number i, thus we use $\widehat{\mathcal{P}}_{i,n}$, $i = 1, 2$ to denote the periodic family $\widehat{\mathcal{P}}$ with the corresponding N_2, i, n; we say that i is the root number and n the class number. Also we stand $O(i, n, x_{20})$ for the orbit in $\widehat{\mathcal{P}}_{i,n}$ with x_{20} coordinate at RC_3.
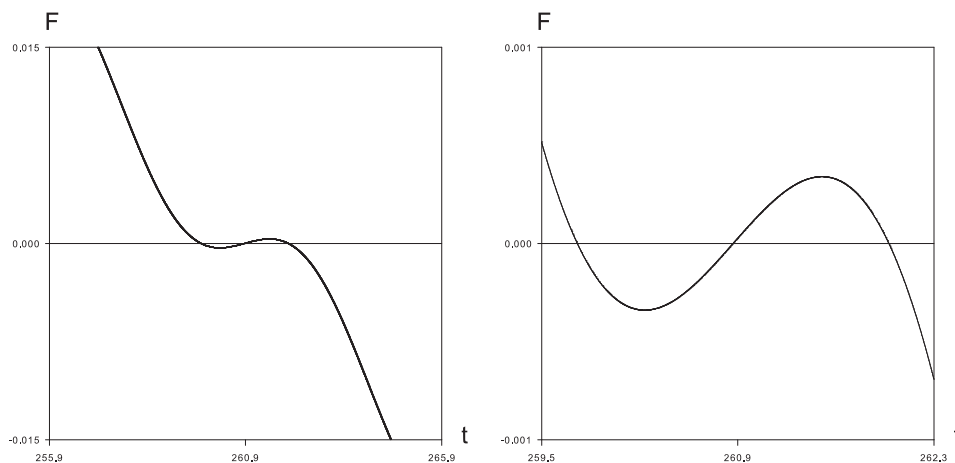
FIGURE 6. An amplified view of F of the orbit $O(2, 41, 0.9997)$, $T_\theta \approx 260.9$.

TABLE 1. Initial conditions vy_{20}, vy_{30}, and values θ, T_θ for the orbits $O(i, n, 0.9997)$, $i = 1, 2$, $n = 41, \cdots, 46$.

i, n	vy_{20}	vy_{30}	θ	T_θ
$1, 41$	1.00033074231	-0.999672669671	6.261056	263.9551723
$1, 42$	1.00039743319	-0.999851955870	6.262949	270.3164151
$1, 43$	1.00023330925	-0.999782352900	6.256888	276.4782610
$1, 44$	1.00030800576	-0.999948704381	6.260236	282.8463259
$1, 45$	1.00015533946	-0.999871704482	6.252373	289.0064551
$1, 46$	1.00023607195	-1.00002723997	6.257733	295.3814054
$2, 41$	1.00040765179	-0.999690533672	3.123549	260.8667477
$2, 42$	1.00038005827	-0.999780710537	3.118758	267.1469371
$2, 43$	1.00030453375	-0.999805643661	3.120520	273.3911836
$2, 44$	1.00028722446	-0.999884233192	3.114997	279.6741658
$2, 45$	1.00022217224	-0.999899629817	3.117557	285.9215129
$2, 46$	1.00021303708	-0.999968625862	3.111125	292.2066777

To depict $\widehat{\mathcal{P}}_{i,n}$, $i = 1, 2$ we choose x_{20} as parameter. Consider the projection of $\widehat{\mathcal{P}}_{i,n}$, $i = 1, 2$ onto the plane (x_{20}, vy_{20}); by moving along the line $x = x_{20}$, for an starting value of vy_{20} big enough, the families are found when vy_{20} decreases. If vy_{20} keeps decreasing and gets a sufficiently small value the families $\widehat{\mathcal{P}}_{i,n}$, $i = 1, 2$ are not longer present and appear the periodic families where the second body follows an inner orbit at the initial time. The description in the plane (x_{20}, vy_{30}) is similar to the one given above, by using vy_{30} instead of vy_{20} in the discussion. In Figures 7, 8 are shown the families $\widehat{\mathcal{P}}_{i,n}$, $i = 1, 2$, $n = 41, \cdots, 46$. Since all the characteristic curves of the periodic families have the same shape, it is enough to plot one point per family to see their distribution (see Figures 9 and 10). The corresponding initial conditions $O(i, n, 0.9997)$ are listed in Table 1.
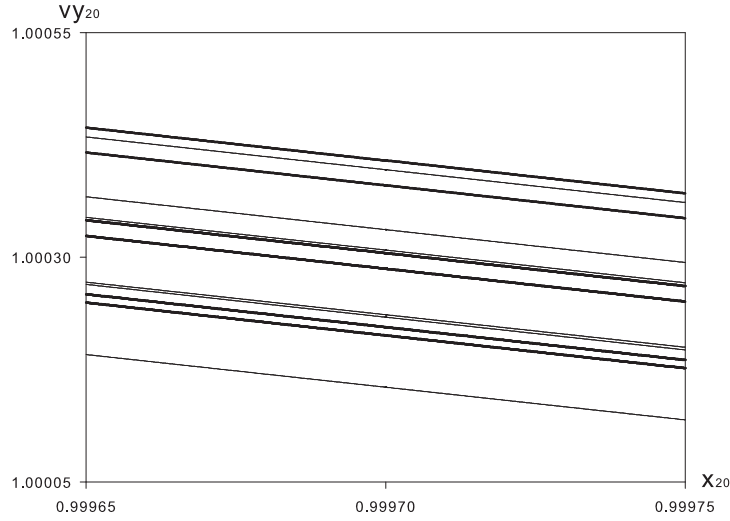
FIGURE 7. Projection of the families $\widehat{\mathcal{P}}_{i,n}$, $i = 1, 2$, $n = 41, \cdots, 46$ onto the plane (x_{20}, vy_{20}). The second root data is denoted by the bold series.
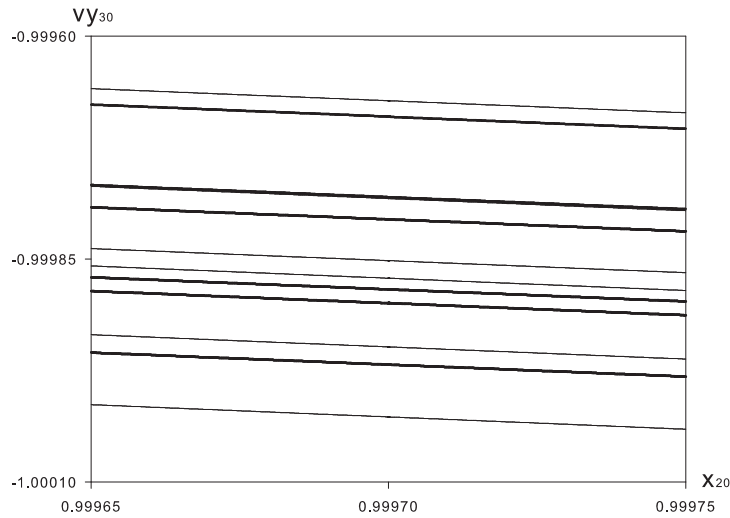

FIGURE 8. Projection of the families $\widehat{\mathcal{P}}_{i,n}$, $i = 1, 2$, $n = 41, \cdots, 46$ onto the plane (x_{20}, vy_{30}). The second root data is denoted by the bold series.

In terms of x_{20}, the times T_θ are increasing functions and the difference between the mean values of T_θ of neighboring families is approximately equal to 2π. The
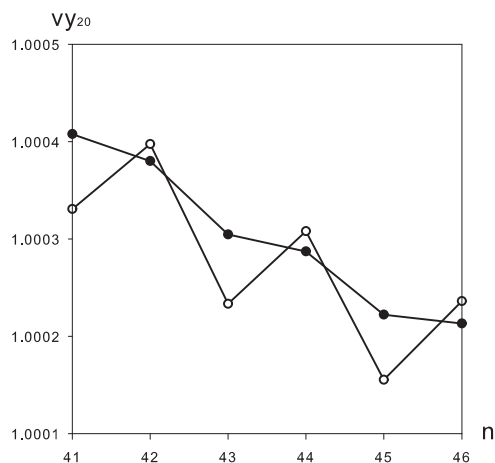
FIGURE 9. Value vy_{20} of the initial conditions of the orbits $O(i, n, 0.9997)$, $i = 1, 2$, $n = 41, \cdots, 46$. The second root data is denoted by the bold series.
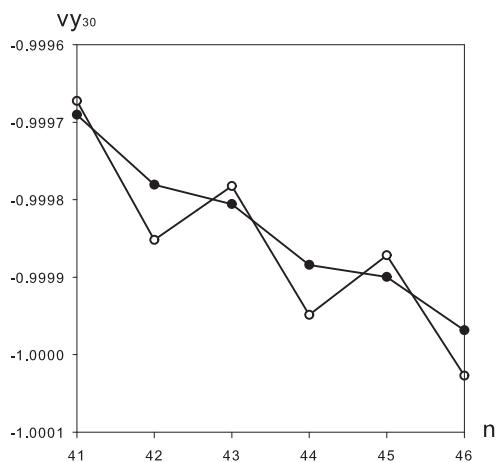

FIGURE 10. Value vy_{30} of the initial conditions of the orbits $O(i, n, 0.9997)$, $i = 1, 2$, $n = 41, \cdots, 46$. The second root data is denoted by the bold series.

first property indicates that in each family the three bodies need more time to come from RC_3 to RC_2 as x_{20} grows. On the other hand, the angle θ can be an increasing or decreasing function of x_{20}. In fact, at least in the studied region, the root and class numbers determine the behavior of θ. Only the families with first root and odd class number present a decreasing angle θ as function of x_{20} (see Figure 11). Concerning the horseshoe orbits belonging to periodic families with increasing or

decreasing θ, we also noticed the following property. For each horseshoe orbit in $\widehat{\mathcal{P}}_{1,n} \cup \widehat{\mathcal{P}}_{2,n}$, $n = 41, \cdots, 46$, and osculating eccentricity e_j of the body $j = 2, 3$ at $t = 0$, holds: if the angle θ decreases (increases) as x_{20} grows then e_2 is less (bigger) than e_3.
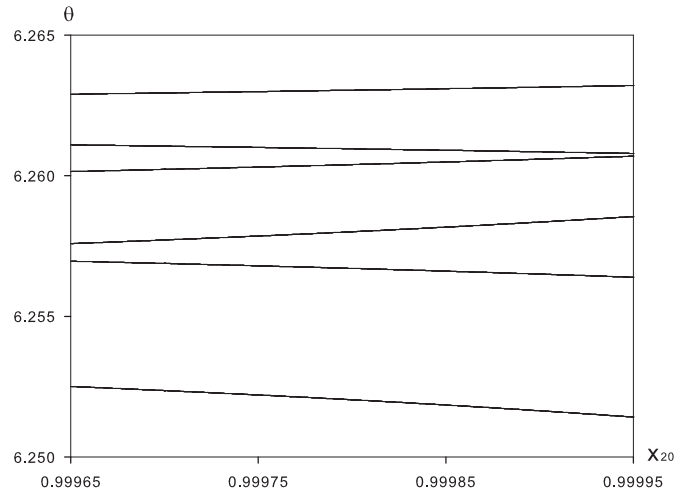

FIGURE 11. Values θ of the families $\widehat{\mathcal{P}}_{1,n}$, $n = 41, \cdots, 46$. At $x_{20} = 0.99965$, from top to bottom the values appear according to the following class numbers: 42, 41, 44, 46, 43, 45.

A rotating frame with an adequate constant angular velocity ω is useful to show symmetric and periodic properties. The position vector $\mathbf{g}$ in the rotating frame is related to its counterpart $\mathbf{r}$ in the inertial frame by means of

$$\mathbf{g} = \begin{pmatrix} \cos(\omega t) & \sin(\omega t) \\ -\sin(\omega t) & \cos(\omega t) \end{pmatrix} \mathbf{r}.$$

Remark 2. Note that in our case the minor bodies carry out an angular displacement equals $2(2n\pi + \theta)$ in a time of $2T_\theta$, then for the orbits in $\widehat{\mathcal{P}}_{i,n}$, $i = 1, 2$, $n = 41, \cdots, 46$ the adequate frequency of the rotation frame is

$$\omega = \frac{2n\pi + \theta}{T_\theta}.$$

In the rotating frame any of these horseshoe orbits is symmetric with respect to the horizontal axis independently of θ, with period equals $2T_\theta$ (see Figure 12).

According to the beginning of this Section, the horseshoe periodic orbits with root number $i = 1$ pass through $N_2 = 1$ configurations C_2 in I_2. From the numerical results it is obtained $N_1 = 3$ (see Figure 13), that is, the periodic families $\widehat{\mathcal{P}}_{i,n}$, $i = 1$, $n = 41, \cdots, 46$ are conformed by horseshoe orbits which pass through $N_1 = 3$ configurations C_3 in I_1 and $N_2 = 1$ configurations C_2 in I_2. In a similar way, the other case is characterized by $i = 2$, $N_1 = 3$, $N_2 = 3$ (see Figure 14).
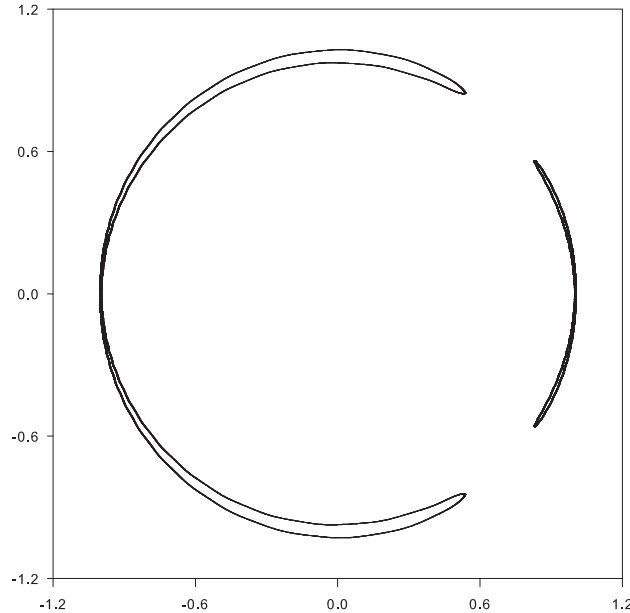
FIGURE 12. Trajectories of the satellites in a rotating frame with constant angular velocity, corresponding to the orbit $O(1, 41, 0.9997)$. The left horseshoe denotes the trajectory of the third body.

To describe the properties of the horseshoe orbits according to their root number, we are going to remember two aspects of the collinear configurations in these orbits. First, the orbits of the minor bodies near collinear configurations are approximately elliptic, since they are relatively distant, and second, at collinear configurations the vectors of position are perpendicular to the vectors of velocity, that is $\mathbf{r}_i \cdot \mathbf{v}_i = \mathbf{0}$, $i = 1, 2, 3$. Therefore the satellites present two types of positions at collinear configurations of the three bodies in the horseshoe orbits: apocentre or pericentre, which we denote respectively by AC and PC. The root number i determines the type of position of the satellites (AC or PC) at RC_3 and RC_2. For reference see Table 2 and Figures 13, 14.

4.6. **Comparison with the case of two equal masses.** In the space of initial conditions $(x_{20}, vy_{20}, vy_{30})$, as function of the class number, the arrangement of $\widehat{\mathcal{P}}_{2,n}$ and the periodic families of Paper I [3], namely $\mathcal{P}_n$, is similar. In contrast, the distribution of the families $\widehat{\mathcal{P}}_{1,n}$ does not show that pattern, and the distance between neighboring families, that is $\widehat{\mathcal{P}}_{i,n}$ and $\widehat{\mathcal{P}}_{i,n+1}$ with $i = 1, 2$, $n = 41, \cdots, 45$, increases and decreases alternately as the class number grows.

The times T_θ of the current work and Paper I present similar features, although they correspond to different reversible configurations: collinear-collinear and collinear-isosceles, respectively.

TABLE 2. Positions of the satellites (apocentre or pericentre, for short respectively AC, PC) at configurations RC_3, RC_2 for horseshoe orbits $O(i, n, x_{20})$ in $\widehat{\mathcal{P}}_{i,n}$, $i = 1, 2$, $n = 41, \cdots, 46$. We stand N_i for the body $N = 2, 3$ whose horseshoe orbit possesses root number i.

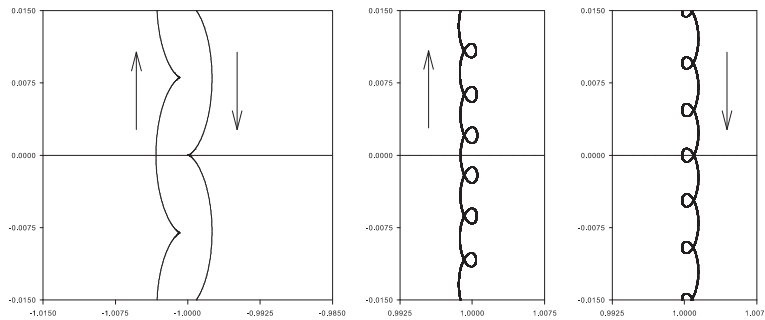| body_root \ configuration	RC_3	RC_2
2_1	PC	PC
3_1	AC	AC
2_2	PC	AC
3_2	AC	PC

FIGURE 13. Trajectories of the minor bodies in a rotating frame with constant angular velocity, corresponding to the orbit $O(1, 41, 0.9997)$. From left to right, the first plot shows the inner and outer trajectories of the body 3, whereas the second and third display respectively the inner and outer trajectories of the body 2 (for reference see Figure 2).

To establish a clear correspondence between the results of both studies, it is useful to remember other issues concerning the periodic families of Paper I. In order to obtain periodic orbits $\mathcal{P}_n$, we used a similar procedure to the one considered here, but instead of RC_2 we chose an isosceles reversible configuration that only exists if at least two of the three masses m_i, $i = 1, 2, 3$ are equal. In the rotating frame these horseshoe orbits have two mirror symmetries, one in each coordinate axis. Due to the vertical symmetry, if the position of the third body at RC_3 is AC (PC) then the position of the second body at RC_2 is AC (PC). Notice that the previous argument is still valid if we interchange the bodies 2 and 3 in the discussion (when both cases are fulfilled we say that property R holds). Finally, evaluating these horseshoe orbits at RC_2 we found that the corresponding root in F is second root. We notice that $\mathcal{P}_n$ and $\widehat{\mathcal{P}}_{2,n}$ share some of the mentioned features. For instance, their horseshoe orbits possess second root and meet property R, which suggests that, in the sense
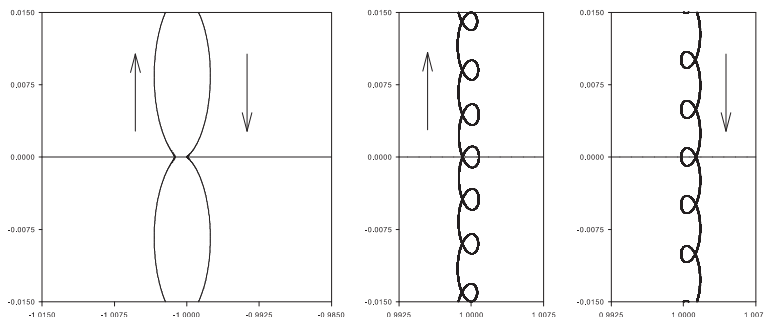
FIGURE 14. Trajectories of the minor bodies in a rotating frame with constant angular velocity, corresponding to the orbit $O(2, 41, 0.9997)$. From left to right, the first plot shows the inner and outer trajectories of the body 3, whereas the second and third display respectively the inner and outer trajectories of the body 2 (for reference see Figure 2).

of Poincare's continuation method of periodic orbits, $\widehat{\mathcal{P}}_{2,n}$ is the continuation of $\mathcal{P}_n$, with $\mu_3 \equiv m_3/m_1$ as the continuation parameter. In Paper I we have used the value $\mu_3 = 3.5 \times 10^{-4}$, then the current value $m_3/m_1 = 9.7 \times 10^{-5}$ can be considered as a perturbation of the first one, that is $\mu_3 + \delta\mu_3$, $\delta\mu_3 = -2.53 \times 10^{-4}$. Under the same reasoning, the families $\widehat{\mathcal{P}}_{1,n}$, whose horseshoe orbits possess one symmetry in the rotating frame, should correspond to the continuation of some periodic families of the case of two equal masses. These families were not calculated in Paper I, since the collinear-isosceles reversible configurations only allow to see horseshoe orbits which possess two symmetries. This is consistent with the fact that, in terms of reversible configurations, collinear-isosceles implies collinear-collinear, nevertheless the converse is not true.

5. **Conclusions.** We have computed and analyzed some periodic families of horseshoe orbits $\widehat{\mathcal{P}}_{i,n}$, $i = 1, 2$, $n = 41, \cdots, 46$. For the numerical study we used the values $m_2/m_1 = 3.5 \times 10^{-4}$, $m_3/m_1 = 9.7 \times 10^{-5}$. Due to the mass ratios used here, the satellites exert an important influence on the planet's movement during the *encounter* (notice that the masses of the satellites are not so small to ignore it, as in the Saturn-Janus-Epimetheus system). Nevertheless, the mass of the planet is enough to avoid an abrupt separation of the satellites during the *encounter* and allow the switch between the role of the small bodies, namely inner or outer. These orbits possess two collinear reversible configurations RC_3, RC_2. Due to this, the horseshoe orbits display a mirror symmetry in the rotating frame.

We conclude mentioning some points that, although have not been studied here, can be approached with the methods of this work. First, it is interesting the study of horseshoe periodic orbits with the usual reversible configuration RC_3 at $t = 0$ and a

second reversible configuration (not necessarily RC_2) that belongs to a later interval I_n, $n > 2$. Second, a question about reversible configurations in the horseshoe orbits. The horseshoe periodic orbits calculated pass through only two different reversible configurations, namely RC_3 at times $t = 2lT_\theta$ and RC_2 at $t = (2l+1)T_\theta$ with $l \in \mathbb{Z}$. An interesting open question in this point is about the existence of horseshoe orbits which pass through more than two different reversible configurations. Finally, with respect to the bifurcation of the families of horseshoe periodic orbits we have noticed that the horseshoe orbits with even number N_2 play an important role, since they are not generic. We have calculated horseshoe periodic orbits with numbers $N_2 = 1$ and $N_2 = 3$, thus apparently the orbits corresponding to $N_2 = 2$ are the bridge between the first ones. It is outlined in Figure 15.
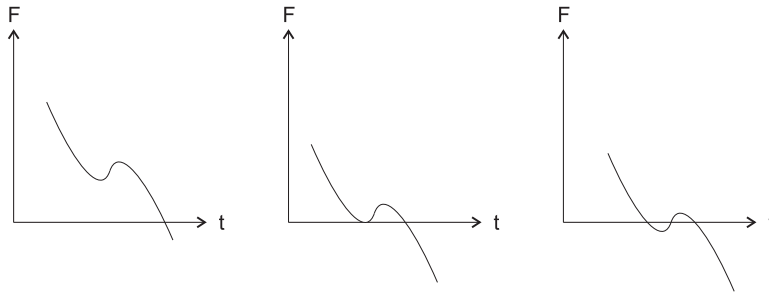

FIGURE 15. Outline of the function F for horseshoe orbits which pass through one, two and three configurations C_2. These cases are shown from left to right, respectively.

Appendix A. **Time-reversal symmetry.** We present some results about the time-reversal symmetries of the equations of motion of the three-body problem (for instance, see [15], [13], [10]).

Consider a solution of the three-body problem

$$\mathbf{r}_i(t), \ \ \mathbf{v}_i(t), \ \ i = 1, 2, 3, \ \ t \in \mathbb{R},$$

with the initial condition $\mathbf{r}_{i0} = \mathbf{r}_i(0)$, $\mathbf{v}_{i0} = \mathbf{v}_i(0)$, $i = 1, 2, 3$, and let K be an orthogonal matrix and $\mathbf{c}$ a vector in $\mathbb{R}^2$. Then

$$\tilde{\mathbf{r}}_i(t) = K\mathbf{r}_i(-t) + \mathbf{c}, \ \ \tilde{\mathbf{v}}_i(t) = -K\mathbf{v}_i(-t), \ \ i = 1, 2, 3, \tag{10}$$

is also a solution of the system with the initial condition $\tilde{\mathbf{r}}_{i0} = K\mathbf{r}_{i0} + \mathbf{c}$, $\tilde{\mathbf{v}}_{i0} = -K\mathbf{v}_{i0}$, $i = 1, 2, 3$.

To see that (10) is a solution of the three-body problem, we calculate the derivatives and show that they satisfy the equations of motion. Using the change of scale $\tau = -t$, we obtain

$$\frac{d}{dt}\tilde{\mathbf{r}}_i(t) = \frac{d}{dt}K\mathbf{r}_i(-t) = -K\frac{d}{d\tau}\mathbf{r}_i(\tau) = -K\mathbf{v}_i(\tau) = \tilde{\mathbf{v}}_i(t).$$

For the velocity of the body i, consider the cyclic values j, k, where $i, j, k \in \{1, 2, 3\}$:

$$\frac{d}{dt}\tilde{\mathbf{v}}_i(t) = -\frac{d}{dt}K\mathbf{v}_i(-t) = K\frac{d}{d\tau}\mathbf{v}_i(\tau) =$$

$$= KG\left[\frac{m_j(\mathbf{r}_j(\tau) - \mathbf{r}_i(\tau))}{|\mathbf{r}_j(\tau) - \mathbf{r}_i(\tau)|^3} + \frac{m_k(\mathbf{r}_k(\tau) - \mathbf{r}_i(\tau))}{|\mathbf{r}_k(\tau) - \mathbf{r}_i(\tau)|^3}\right] =$$

$$= \frac{Gm_j(\tilde{\mathbf{r}}_j(t) - \tilde{\mathbf{r}}_i(t))}{|\mathbf{r}_j(\tau) - \mathbf{r}_i(\tau)|^3} + \frac{Gm_k(\tilde{\mathbf{r}}_k(t) - \tilde{\mathbf{r}}_i(t))}{|\mathbf{r}_k(\tau) - \mathbf{r}_i(\tau)|^3}.$$

We also use the invariance of the norm under the matrix multiplication of K:

$$|\mathbf{r}_s(\tau) - \mathbf{r}_i(\tau)| = |K(\mathbf{r}_s(\tau) - \mathbf{r}_i(\tau))| = |\tilde{\mathbf{r}}_s(t) - \tilde{\mathbf{r}}_i(t)| = \tilde{r}_{is},$$

therefore

$$\frac{d}{dt}\tilde{\mathbf{v}}_i(t) = \frac{Gm_j(\tilde{\mathbf{r}}_j(t) - \tilde{\mathbf{r}}_i(t))}{\tilde{r}_{ij}^3} + \frac{Gm_k(\tilde{\mathbf{r}}_k(t) - \tilde{\mathbf{r}}_i(t))}{\tilde{r}_{ik}^3}.$$

A.1. **Collinear reversible configurations.** In the following we use

$$K = \begin{pmatrix} 1 & 0 \\ 0 & -1 \end{pmatrix}, \quad \mathbf{c} = \mathbf{0}.$$

Notice that if

$$\tilde{\mathbf{r}}_{i0} = \mathbf{r}_{i0}, \quad \tilde{\mathbf{v}}_{i0} = \mathbf{v}_{i0}, \quad i = 1, 2, 3 \tag{11}$$

is fulfilled then, as a consequence of the uniqueness of the solution and (10), we have $\mathbf{r}_i(t) = K\mathbf{r}_i(-t)$, $\mathbf{v}_i(t) = -K\mathbf{v}_i(-t)$, $i = 1, 2, 3$. Solving the system (11) we obtain

$$y_{i0} = 0, \quad v_{xi0} = 0, \quad i = 1, 2, 3,$$

that is, the initial condition corresponds to a collinear reversible configuration (see Figure 16). We remark that if the collinear reversible configuration happens at $t = \alpha$, instead of $t = 0$, then $\mathbf{r}_i(t) = K\mathbf{r}_i(2\alpha - t)$, $\mathbf{v}_i(t) = -K\mathbf{v}_i(2\alpha - t)$, $i = 1, 2, 3$ holds.
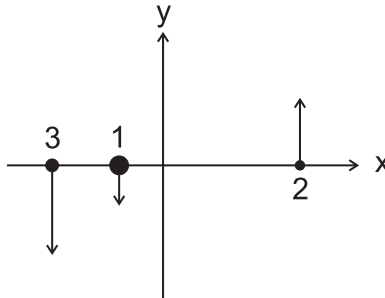

FIGURE 16. Collinear reversible configuration.

REFERENCES

[1] E. Barrabés and S. Mikkola, *Families of periodic horseshoe orbits in the restricted three-body problem*, Astron, Astrophys, **432** (2005), 1115–1129.

[2] A. Bengochea and E. Piña, *The Saturn, Janus and Epimetheus dynamics as a gravitational three-body problem in the plane*, Rev. Mexicana Fís., **55** (2009), 97–105.

[3] A. Bengochea, M. Falconi and E. Pérez-Chavela, *Symmetric horseshoe periodic orbits in the general planar three-body problem*, Astrophys. Space Sci., **333** (2011), 399–408.

[4] J. M. Cors and G. R. Hall, *Coorbital periodic orbits in the three body problem*, SIAM J. Appl. Dyn. Syst., **2** (2003), 219–237.

[5] S. F. Dermott and C. D. Murray, *The dynamics of tadpole and horseshoe orbits. I. Theory*, Icarus, **48** (1981), 1–11.

[6] S. F. Dermott and C. D. Murray, *The dynamics of tadpole and horseshoe orbits. II. The coorbital satellites of Saturn*, Icarus, **48** (1981), 12–22.

[7] J. R. Dormand and P. J. Prince, *A family of embedded Runge-Kutta formulae*, J. Comput. Appl. Math., **6** (1980), 19–26.

[8] M. Hénon and J. M. Petit, *Series expansion of encounter-type solutions of Hill's problem*, Celest. Mech. Dynam. Astron., **38** (1986), 67–100.

[9] X. Y. Hou and L. Liu, *The symmetric horseshoe periodic families and the lyapunov planar family around L_3*, Astron. J., **136** (2008), 67–75.

[10] J. S. W. Lamb and J. A. G. Roberts, *Time-reversal symmetry in dynamical systems: A survey*, Phys. D, **112** (1998), 1–39.

[11] J. Llibre and M. Ollé, *The motion of Saturn coorbital satellites in the restricted three-body problem*, Astron. Astrophys, **378** (2001), 1087–1099.

[12] K. R. Meyer and G. R. Hall, "Introduction to Hamiltonian Dynamical Systems and the N-Body Problem," 1st edition, Springer-Verlag, New York, 1992.

[13] F. J. Muñoz-Almaraz, J. Galán and E. Freire, *Families of symmetric periodic orbits in the three body problem and the figure eight*, Monogr. Real Acad. Ci. Exact. Fís.-Quím. Nat. Zaragoza, **25** (2004), 229–240.

[14] J. M. Petit and M. Hénon, *Satellite encounters*, Icarus, **66** (1986), 536–555.

[15] A. E. Roy and M. W. Ovenden, *On the occurrence of commensurable mean motions in the solar system. II. The mirror theorem*, Mon. Not. R. Astron. Soc., **115** (1955), 296–309.

[16] F. Spirig and J. Waldvogel, *The three-body problem with two small masses: A singular-perturbation approach to the problem of Saturn's coorbiting satellites*, in "Stability of the Solar System and its Minor Natural and Artificial Bodies," (ed. V. G. Szebehely), Reidel, (1985), 53–63.

[17] C. F. Yoder, G. Colombo, S. P. Synnott and K. A. Yoder, *Theory of motion of Saturn's coorbiting satellites*, Icarus, **53** (1983), 431–443.

[18] C. F. Yoder, S. P. Synnott and H. Salo, *Orbits and masses of Saturn's co-orbiting satellites, Janus and Epimetheus*, Astron. J., **98** (1989), 1875–1889.

[19] J. Waldvogel and F. Spirig, *Co-orbital satellites and hill's lunar problem*, in "Long-Term Dynamical Behaviour of Natural and Artificial N-Body Systems" (ed. A. E. Roy), Kluwer, (1988), 223–234.

E-mail address: bengochea@ciencias.unam.mx
E-mail address: falconi@servidor.unam.mx
E-mail address: epc@xanum.uam.mx